First-principles studies of the thermodynamic properties of bulk Li

1997 J. Phys.: Condens. Matter 9 2135

(http://iopscience.iop.org/0953-8984/9/10/004)

J. Phys.: Condens. Matter **9** (1997) 2135–2148. Printed in the UK PII: S0953-8984(97)79022-2

First-principles studies of the thermodynamic properties of bulk Li

P Staikov, A Kara and T S Rahman

Department of Physics, Cardwell Hall, Kansas State University, Manhattan, KS 66506, USA

Received 29 October 1996

Abstract. We have calculated the electronic structure and the vibrational properties of bulk Li in the fcc and bcc structures using large super-cells and an *ab initio*, non-local pseudopotential approach with a plane-wave expansion. The method is based on the density functional theory with core corrections and local exchange and correlation effects. The calculated phonon dispersion curves for the bcc structure are compared with the neutron scattering data. The difference between the Helmholtz free energies for the bcc and the closed-packed structures, in the harmonic approximation, is found to be small for the temperature range of interest. The zero-point energies for both structures are substantial, while the heat capacity differential displays a switch at around 90 K.

1. Introduction

Lithium, the lightest metal with a simple elemental electronic configuration and a broad range of practical applications, has naturally been the subject of both theoretical and experimental investigations for a long time. Yet its electronic and structural properties remain enigmatic to this day. Like other alkali metals it has a bcc room temperature structure, and at low temperatures it undergoes a structural transformation. For lithium the low-temperature phases have led to puzzlement and contradictions. Very early on Barrett and Trautz [1] had suggested that below 70 K the phase was hexagonal close-packed. Later, on the basis of additional data [2], Overhauser [3] proposed that the low-temperature phase was characterized by a nine-layer sequence of close-packed planes (ABCBCACAB) called 9R. This structure was subsequently identified in several sets of neutron scattering data [4]. More recently, analysis of diffuse neutron scattering data [5] has led to the opinion that below 80 K a disordered polytype structure, consisting of the short-range correlated fcc and hcp phases, coexists with the longer-ranged, ordered 9R structure.

The large deviations in the observed properties of bulk Li from nearly-free-electron behaviour (for example, the lack of superconductivity at very low temperatures) have led to several sophisticated theoretical studies of its electronic structure, which have focused on band-structure effects involving contributions of electron–phonon and electron–electron interactions [6], and calculations of the total energy [7] and the electron–phonon coupling constant [8]. The issue of the martensitic transformation [9–11] has also been broached and, the bulk phonon dispersion curves for the bcc structure have been calculated using phenomenological methods [12], as well as *ab initio* electronic structure techniques [13–18]. While these efforts have been very useful in identifying various aspects of the electronic and structural behaviour of lithium, the driving force for the martensitic transformation is not yet

0953-8984/97/102135+14$19.50

understood. The analysis of the bulk phonon dispersion even with the most sophisticated of theoretical techniques has not as yet addressed the issue of this structural phase transition. In fact, the phonon dispersion curve calculated by Frank *et al* does not produce a reasonable fit to experimental data for the bcc phase without invoking a global shift of 16% in calculated frequencies, leading to questions about the applicability of these sophisticated theoretical methods to explore the structure and the dynamics of bulk Li.

Many years ago it was suggested that in martensitic transitions, in general, vibrational entropy may play an important role in stabilizing the higher-temperature phase [19–21]. In the case of lithium, this idea was pursued by Bajpai *et al* [11] whose calculations were based on modified Hartree–Fock equations and the self-consistent pseudopotential method [22] as applied to lattice dynamics [23]. These authors were able to display that under certain assumptions their model calculations led to the observed close-packed–bcc transition for bulk lithium at temperatures reasonably close to the experimental ones. However, as these calculations were not based on first principles, their reliability and predictive capacity have remained open to question.

The aim of this paper is to calculate the thermodynamic properties of bulk Li and to examine the contribution of the vibrational free energy and entropy to the stability of the proposed structures as a function of temperature. By using as accurate a method as is currently feasible for the calculations of the structural and dynamical properties of Li, we also address the issue of the applicability of these theoretical techniques in distinguishing between structures that remain very close in energy even when dynamic effects are included. The theoretical technique that we employ for the purpose is an *ab initio*, non-local pseudopotential method [24] based on the density functional theory [25, 26] with the local density approximation (DFT/LDA) and using the plane-wave representation [27]. The usage of an iterative diagonalization scheme with a preconditioned steepest-descent method [28, 29] allows us to consider systems with over a hundred atoms in the super-cell, which is necessary in order to include interactions extending to several neighbours for the calculations of the phonon density of states. This method is in essence along the same lines as that of Frank *et al* [13] save for variations in some technical details, with the major difference that we calculate the dispersion of the bulk phonons and the density of states for not just the bcc but also the fcc structure. In addition, we evaluate the thermodynamic properties of these structures in the temperature range, 0 K–150 K, during which the martensitic transition is reported to occur. Our calculated structural energy differences thus include dynamical effects even at $T = 0$ K (zero-point energy) and allow us to examine the applicability of DFT/LDA calculations in extracting the relative differences in the free energies of two structures at finite temperatures. To our knowledge this is the first calculation of the thermodynamic properties of bcc and fcc Li based on DFT/LDA.

Our choice of the fcc phase as representative of the coexistent close-packed structures needs a little clarification. Since 9R is the predominant low-temperature phase it would seem natural to choose it for comparison with the higher-temperature bcc phase. However, apart from the fact that the fcc structure, with fewer atoms per unit cell, is easier to handle than the 9R structure vis-à-vis the total energy calculation, we find that it has the lowest static, total energy at zero temperature. Also, according to Schwarz and Blaschko [5] the preference of the 9R structure is most likely the result of the relief of a macroscopic shear which arises with the formation of an fcc nucleus within a bcc crystal. The 9R structure may thus be viewed as a fcc lattice with a stacking fault after each ABC sequence which leads to a large reduction of the macroscopic shear in the original fcc lattice. Thus the choice of fcc as the low-temperature phase is quite reasonable. In the next section we present some details of the theoretical calculations for the total energy, the force-constant

matrix and the thermodynamic functions. This is followed in section 3 with results, while section 4 contains some concluding remarks.

2. Theoretical details

Our calculations of the electronic structure of metallic Li are based on the density functional theory in the local density approximation [25–27]. We use a plane-wave, pseudopotential technique to solve the Kohn–Sham equations with the exchange–correlation energy given by the Vosko–Wilk–Nusair [30, 31] parametrization. The pseudopotential employed is soft, non-local and of the form supplied by Troullier and Martins [32]. A partial core correction [33] is also included to account for the contribution of the core to the exchange–correlation energy. The sampling of the Brillouin zone (BZ) is performed according to the Monkhorst–Pack [34] scheme and the symmetry of the lattice is used to reduce the number of special k-point sets to the irreducible part of the BZ. Next, the iterative diagonalization scheme with a preconditioned steepest-descent algorithm, in which the step along the direction of steepest descent is inversely proportional to the kinetic energy of the state [29], is used. This procedure has been found to lead to convergence very efficiently in studies of bulk Al and Mg [29]. For sufficiently large k-point samplings, the energy functional that we minimize gives the electronic contribution to the free energy, F_{el}, for different values of the Fermi broadening k_BT, quite accurately [35].

We test the above recipe for the electronic structure calculations by first evaluating some of the structural properties of bulk Li using standard procedures with one atom/unit cell. First we check the dependence of the results on k-point sampling, and on the choice of the energy cut-off employed in the calculation of the number of plane waves. We then proceed with the calculation of the total energy and force-constant matrix using a large number of atoms in the super-cell—the number of atoms being dictated by the range of interaction necessary for the evaluation of the force-constant matrices, needed for the evaluation of the phonon dispersion.

As has been nicely summarized by Frank *et al* [13] there are several methods for calculating the phonon dispersion curves: linear response theory and the direct method. We refer the reader to their work for a comparison of these methods. To calculate the elements of the force-constant matrix, we have chosen the so-called *direct approach* [36, 13], in which the force constants are computed from the Hellmann–Feynman forces [37] resulting from appropriate displacements of atoms in the super-cell. Apart from being intuitively appealing, an advantage of this method is that the electronic structure calculation has to be carried out for only a few displacements of atoms in the super-cell. For example, for the case of cubic crystals just one calculation of the Hellmann–Feynman forces may be sufficient to recover all force constants, after considerations of the symmetry of the system. The direct method also has a large range of applicability. For example, in the calculations of the vibrational spectra of defects in solids, methods like those based on linear response theory are not suitable. A possible limitation of the method is that an increase in the range of the interaction leads to a corresponding increase in the size of the super-cell. This is particularly annoying for systems in which interactions do not die off quickly with distant neighbours. However, if the super-cell becomes unreasonably large, a slightly different approach can be applied. By displacing entire planes of atoms the interplanar force constants can be obtained from significantly smaller sizes of super-cell. Since the interplanar force constants are linear combinations of interatomic ones, the latter may then be extracted using a finite set of linear equations [38]. Once the full force-constant matrix is available, calculations of phonon dispersion curves and the vibrational density of states is straightforward. These

densities of states can then be used for the computation of thermodynamic quantities.

To illustrate the direct method, suppose that the atom at lattice position $\boldsymbol{R}$ has a displacement $u_\alpha(\boldsymbol{R})$, along the Cartesian direction α. A component of the force acting on this atom, along direction β, is given by

$$F_\beta(\boldsymbol{R}) = -\sum_{\alpha \boldsymbol{R}'} \Phi_{\beta\alpha}(\boldsymbol{R}, \boldsymbol{R}')u_\alpha(\boldsymbol{R}') \tag{1}$$

where $\Phi_{\beta\alpha}$ is the force constant in question. Now if only one of the displacements, say $u_x(0)$, is taken to be non-zero, equation (1) simplifies significantly. The displacement of the centre atom in the x-direction would then cause forces $\boldsymbol{F}(\boldsymbol{R})$ to act on the rest of the atoms in the super-cell. The xth column of the force-constant matrix can now be determined from

$$\Phi_{x\beta}(0, \boldsymbol{R}) = -\frac{F_\beta(\boldsymbol{R})}{u_x(0)} \tag{2}$$

where $u_x(0)$ is the displacement of the centre atom. Here we have chosen $u_x(0)$ to be sufficiently small (1% of the lattice constant), and eliminated cubic and quartic terms in the expansion of the potential, by performing electronic structure calculations with displacements $-u_x(0)$ and $2u_x(0)$ and manipulating the three expressions so obtained.

It should be pointed out that there is another technical reason for equation (2) to be only approximately true. As a result of lattice periodicity, the centre atom in the neighbour cells are also displaced and contribute to the forces acting on the atoms in the cell under consideration. In order to make this contribution negligible, the size of the super-cell should be such that the smallest distance from the displaced atom to the cell boundary is larger than the assumed range of interaction. For example, for a 54-atom, bcc cell, the fourth neighbour of the centre atom is on the cell boundary and should not be included in the calculation because it is equally influenced by the displaced atoms in two cells leading to artificial cancellation of forces. Similarly, although the fifth neighbour is contained in the super-cell it should be also excluded since its inclusion would be inconsistent with the exclusion of the fourth neighbour. Thus a bcc super-cell of 54 atoms can consist of coupling just to the third neighbour. In the case of lithium we found that interactions up to fifth neighbours had to be incorporated to give reliably converged results for the phonon frequencies. Consequently, for the bcc structure the number of atoms in the super-cell was taken to be 128. For the fcc structure the corresponding number is 108 per super-cell, which ensures coupling up to the fourth neighbour.

Once $\Phi_{x\beta}(0, \boldsymbol{R})$ is determined, one can find $\Phi_{y\beta}(0, \boldsymbol{R})$ and $\Phi_{z\beta}(0, \boldsymbol{R})$, using transformation rules after the crystal is subjected to an operation S from its space group:

$$\Phi_{\alpha\beta}(0, \boldsymbol{R}) = \sum_{\lambda\mu} S_{\alpha\lambda} S_{\beta\mu} \Phi_{\lambda\mu}(0, \boldsymbol{R}). \tag{3}$$

Note that for cubic crystals it is sufficient to apply rotations of $\pi/2$ around the y- and z-axes to get the remaining force constants. The Fourier transform of the force-constant matrix finally yields the dynamical matrix

$$D_{\alpha\beta}(\boldsymbol{q}) = \sum_{\boldsymbol{R}} \frac{1}{M} \Phi_{\alpha\beta}(0, \boldsymbol{R}) \mathrm{e}^{\mathrm{i}\boldsymbol{q}\cdot\boldsymbol{R}} \tag{4}$$

where M is the ion mass. By diagonalizing $D_{\alpha\beta}(\boldsymbol{q})$ for a set of $\boldsymbol{q}$s, we derive the dispersion $\omega(\boldsymbol{q})$. To evaluate the vibrational density of states from the calculated phonon dispersion curves, a simple root sampling technique [39] is used. We find that to obtain a smooth shape for the density of states, a sampling of around 10^6 points in the irreducible part of the Brillouin zone is needed. Using these densities of states, $N(\omega)$, we compute the vibrational

contribution to the free energy as a function of temperature, in the harmonic approximation. The Helmholtz free energy is given by

$$F(T) = F_{el}(T) + F_{vib}(T) \tag{5}$$

with

$$F_{vib}(T) = k_B T \int_0^\infty N(\omega) \ln\left[2\sinh\left(\frac{\hbar\omega}{2kT}\right)\right] \mathrm{d}\omega \tag{6}$$

and $F_{el}(T)$ is the electronic contribution to the free energy.

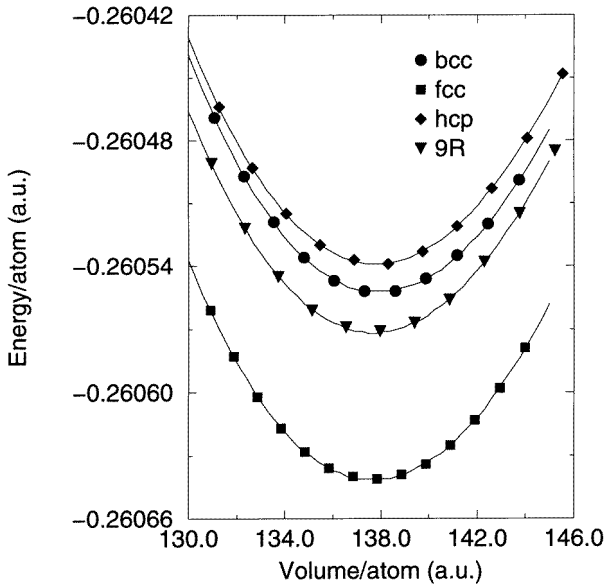

Figure 1. The total energy per atom plotted as a function of the volume for four different structures, bcc, fcc, hcp, and 9R. The curves are obtained by fitting the points through the Murnaghan equation of state as in reference [47].

3. Results and discussion

The calculated zero-temperature, static, total energies per atom, as functions of the crystal volume per atom, for Li in the four proposed structures bcc, fcc, hcp and 9R, are presented in figure 1. There are a number of similar calculations already available in the literature and the results of almost all of them differ in one way or another. Like Boettger and Trickey [40], for example, we find fcc to be the most stable phase. However, the energy difference between the fcc and the bcc structures is only 2.4 meV in our results, compared to 8.2 meV in their work. The relative order of the phases that we obtain is different from the one from a similar plane-wave, pseudopotential calculation presented by Dacorogna and Cohen [7]. However, as pointed out in that work the energy differences are very small, and within the minimum convergence criterion reasonable for the theory. To ensure that our calculation is accurate, we have insisted that any further increase of the energy cut-off radius or the number of the special k-points leads to changes in total energy that are smaller than the energy differences between the phases. This has led to a choice of $E_{cut} = 22$ Ryd

and 68, 60, 144, and 110 special k-points in the irreducible BZ for the bcc, fcc, hcp and 9R structures, respectively, to yield the results presented in figure 1. Somewhat surprisingly we find that the hcp structure is highest in energy. It is interesting to note that with a k-point sampling of 40 special k-points in the irreducible BZ (the one used by Dacorogna and Cohen [7]) we also find the structural energy of the hcp structure to be lower than that of the bcc structure. Finer sampling of the Brillouin zone gives a slightly higher energy of the hcp phase (0.4 meV above the bcc curve in figure 1). Our conclusion here is that for smaller values of E_{cut} (<22 Ryd) the exact ordering of the four structures for bulk Li depends on the choice of k-point sampling. In general the energy cut-off and the number of k-points that we use are higher than in any other study that we are aware of, allowing us to believe that our calculation is quite accurate, within the usage of *ab initio* pseudopotentials and LDA. It is also worth noting, however, that the small energy differences found for the different phases are consistent with the fact that all of these phases coexist at low temperatures. In table 1, we report our calculated values for the lattice constant a_0, the bulk modulus B_0, and the pressure derivative of the bulk modulus B_0' of bulk Li, together with results from other theoretical calculations and experimental data.

Table 1. Structural properties of bulk Li in comparison with other theoretical calculations and experimental data. For the hcp structure we find $c/a = 1.62$. For 9R we assume the ideal close-packing c/a ratio.

	Structure	a_0 (au)	B_0 (kbar)	B_0'
Boettger and Trickey [40]	fcc	8.23	187	
	bcc	6.60	147	
Dacorogna and Cohen [7]	hcp	5.71	137	3.3
	fcc	8.09	138	3.4
	bcc	6.43	130	2.6
Present calculation	hcp	5.83	133	3.3
	fcc	8.20	134	2.8
	bcc	6.51	135	3.5
	9R	5.80	133	3.4
Experiment [46]	bcc	6.60	116	
Experiment [1]	hcp	5.88	126.5	

The calculated phonon dispersion curves for the bcc and the fcc phases are presented in figures 2 and 3, respectively. The super-cells used for the dynamical calculations consisted of 128 atoms for the bcc structure and 108 atoms for the fcc structure. This corresponds to coupling to the fifth neighbour in the bcc, and to the fourth neighbour in the fcc structure. With this large a super-cell, the energy cut-off of 22 Ryd makes the calculation prohibitively large. We, therefore, had to restrict ourselves to a smaller energy cut-off in order to make the calculations tractable. From an analysis of the sensitivity of the calculated phonon frequencies to the choice of the cut-off energy, we found $E_{cut} = 12$ Ryd to yield reasonable results. To test the reliability of the phonon frequencies arising from the smaller energy cut-off, we compared the values at specific points of the Brillouin zone using the frozen-phonon method and energy cut-offs of 12 Ryd and 22 Ryd. The results are presented in table 2. Since the frozen-phonon calculation does not limit the interactions to a finite number of neighbours, the values in the table indicate that the choice of the size of our super-cells is reasonable. In the present calculation, eight k-points in the BZ, equivalent to one special k-point in the irreducible BZ, were sampled. The adequacy of the k-point sampling was checked for the 54 atom super-cell in which we found that the force constants, calculated

with four special k-points in the irreducible BZ, were the same within 3% as the ones calculated with one special k-point. A related issue is the value of the lattice constant for the two choices of E_{cut}. To ensure the consistency of our method we calculated a_0 once more with a cubic unit cell with two atoms, $E_{cut} = 12$ Ryd, and the k-point sampling equivalent to that used for the case of the 128-atom cell. The value of the lattice constant was only 0.1% different from the one already calculated. To be able to calculate stable Hellmann–Feynman forces we allow for partial occupation of the electronic states which were taken to follow the Fermi distribution with a temperature broadening $k_BT = 0.01$ au. For the earlier calculations of the total energy, this parameter was taken to be 0.001 au. The higher value of k_BT in the force calculation gives better convergence and does not affect the values of the calculated density functional forces [35].

Table 2. Phonon frequencies at specific points in the Brillouin zone from different calculations.

Type of calculation	E_{cut} (Ryd)	Mode	f (THz)
bcc, N point			
From atomic force constants	12	L	9.95
		T1	2.43
		T2	6.32
Frozen phonon	12	L	9.72
		T1	2.20
		T2	6.10
Frozen phonon	22	L	9.68
		T1	2.20
		T2	6.16
Experimental results [41]		L	9.0
		T1	1.9
		T2	5.7
fcc, X point			
From atomic force constants	12	L	10.48
		T	7.41
Frozen phonon	22	L	10.24
		T	7.12
Frozen phonon	12	L	10.14
		T	6.95

The calculated dispersion curves for the bcc phase are compared to the experimental values measured at 98 K [41], in figure 2(a). The calculation reproduces the shape of the dispersion curves very well but the calculated values differ from the experimental ones by a factor of about 1.10 at the zone boundaries. This result is similar to that of Frank *et al* [13] who needed a scaling factor of 1.16 to get an agreement with the experimental data. Perhaps a reason for this discrepancy is the error that the LDA introduces in estimating lattice constants. We calculate a value of 6.51 au for the lattice constant, which is larger than 6.34 au given by Frank *et al*, but is still about 1% smaller than the experimental value of 6.60 au [46]. In figure 2(b), we replot the dispersion curves for the bcc structure with a rescaling of the calculated curves by a factor of 0.9, in a manner similar to that of Frank *et al* [13]. The fit to the experimental data is now deceptively good in most parts of the Brillouin zone. The low-frequency mode (T1) along the [110] direction, however,

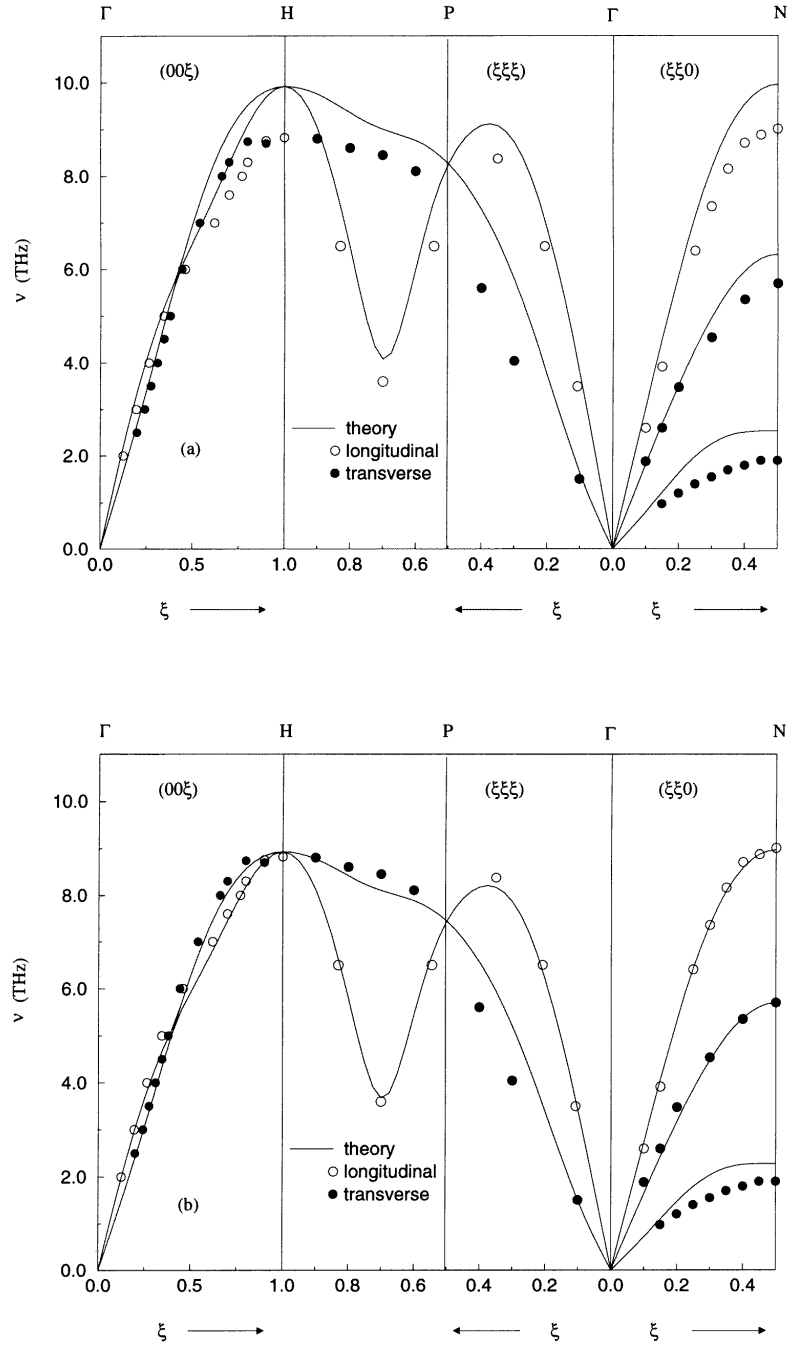

Figure 2. Phonon dispersion curves for bcc Li along high-symmetry directions. Symbols represent experimental data from reference [41] and the solid line is from the present calculations: (a) unscaled values; (b) calculated frequencies scaled by a factor of 0.9. Here ξ is the reduced wave vector.

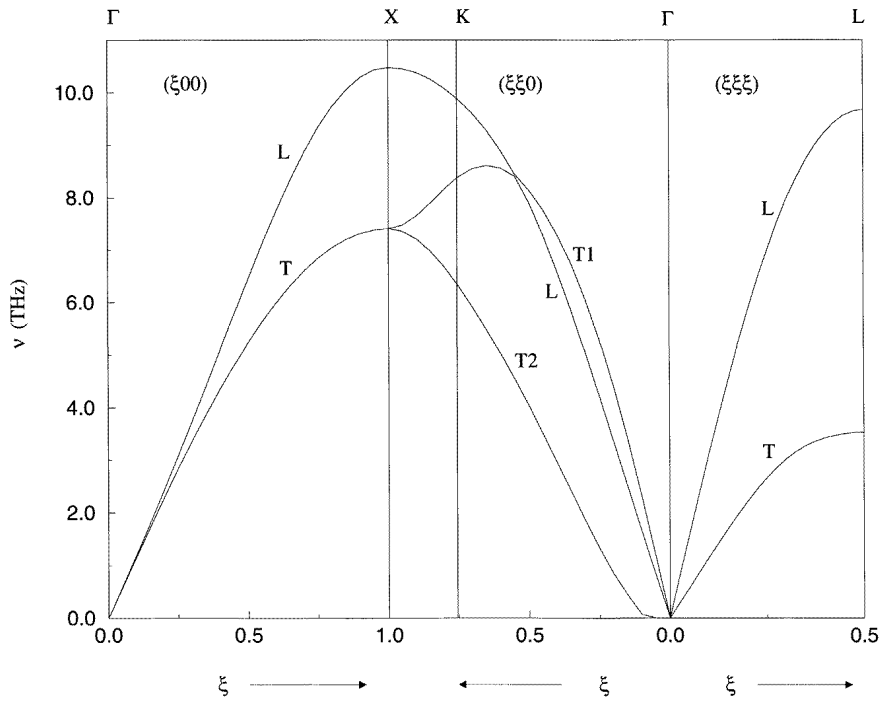

Figure 3. Calculated phonon dispersion curves for fcc Li in the high-symmetry directions.

is still noticeably stiffer than that in the experimental data. Meanwhile, the shapes of the dispersion curves in figure 3, for the fcc structure of bulk Li, compare well to a Hartree–Fock calculation [11] and resemble the dispersion curves of other fcc metals [41]. At the moment there are no low-temperature (below 80 K) phonon data available to compare with the dispersion curves in figure 3.

It may be argued that a smaller value for the lattice constant results in stiffer force constants, and overall higher phonon frequencies. This would imply that the discrepancy between the theoretical calculations and the experimental data in figure 2(a) is mainly due to the difference in the lattice constants. To check the validity of such a rationale, we carried out a set of calculations in which the lattice constant for the bcc structure was taken to be the same as in the experimental data. The resulting phonon dispersion curve along [110] is shown in figure 4. Contrary to one's expectations the frequencies of the modes do not change significantly. This means that the interactions between the ions cannot be softened simply by increasing the distance between them. It also implies that the LDA error in obtaining the lattice constant is not the main reason for the deviation of the calculated phonon frequencies from those in the experiment. Another interesting feature in figure 4 is that the frequency of the shear T1 phonon mode increases on increasing the lattice constant by a small amount. This suggests that the Grüneisen parameter is negative and there may be softening of this mode and a possible structural phase transition at higher pressure [39]. We are not in a position to document this aspect any further.

The calculated vibrational DOS for fcc and bcc lithium are presented in figure 5. They are obtained through sampling of about 10^6 points in the irreducible part of the BZ, which is computationally quite feasible. Using the computed DOS, the Helmholtz free energies

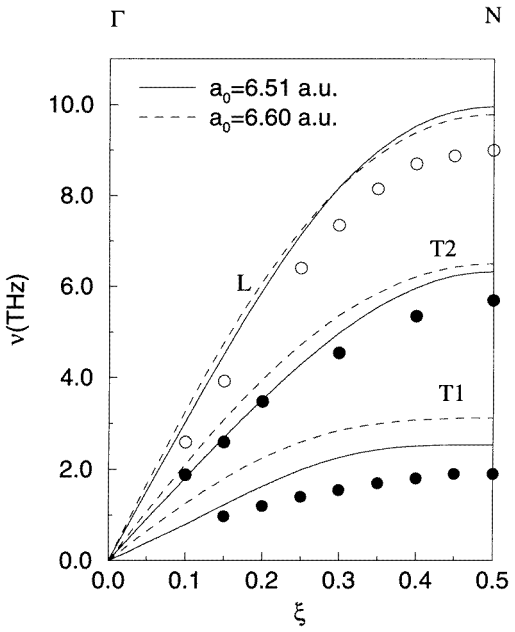

Figure 4. Phonon dispersion along [110] calculated for two different values of the lattice constant: $a_0 = 6.51$ au (present calculation) and $a_0 = 6.60$ au (experimental data). Symbols represent experimental data from reference [41].

and the lattice heat capacities for the two structures are calculated. The difference in the lattice specific heats of the fcc and bcc phases is shown in figure 6. An interesting feature in figure 6 is the switch in the heat capacity differential at around 90 K. At temperatures below 90 K, the lattice heat capacity of the bcc structure is higher and above that temperature it is lower. This hint of a possible preference for one of the structures is, however, not borne out by the calculated vibrational free energies, obtained using equation (6), with the electronic contribution F_{el} added and plotted in figure 7. We find F_{el} to be significantly smaller than F_{vib}. As can be seen in figure 7, the curves do not intersect and do not exhibit any phase transition at least up to temperatures of several hundred degrees. Of course, the difference between the free energies is so small that even if the curves crossed it would have been difficult to arrive at an unambiguous result for the role of the vibrational entropy in the phase transition. A useful aside here comes from the zero-point motion which can be calculated easily from the vibrational density of states. We find the zero-point energy for the bcc structure to be 46.9 meV and for the fcc phase it is 44.5 meV. The magnitude of the zero-point motion is greater than the differences between the static energies or the free energies. This suggests that for a light metal like Li it is essential to take the zero-point motion into account in any discussion of the energetics.

4. Concluding remarks

Our aim in this paper was to examine the free energy of bulk Li in the bcc and the closed-packed structure (here chosen to be fcc) as a function of temperature, using accurate calculations of the total energy and the phonon density of states. The free energies were

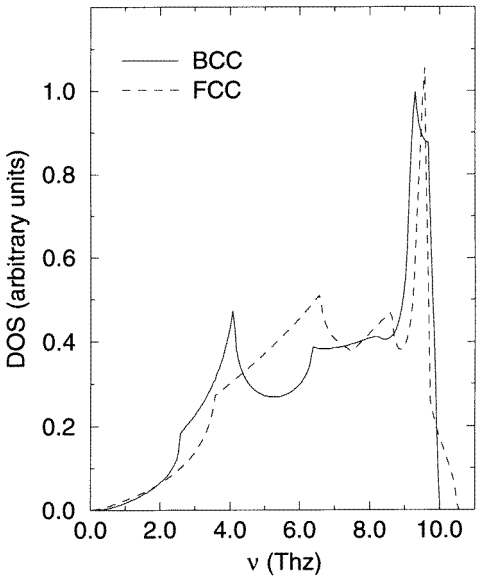

Figure 5. Vibrational densities of states for lithium in the bcc and fcc structures.

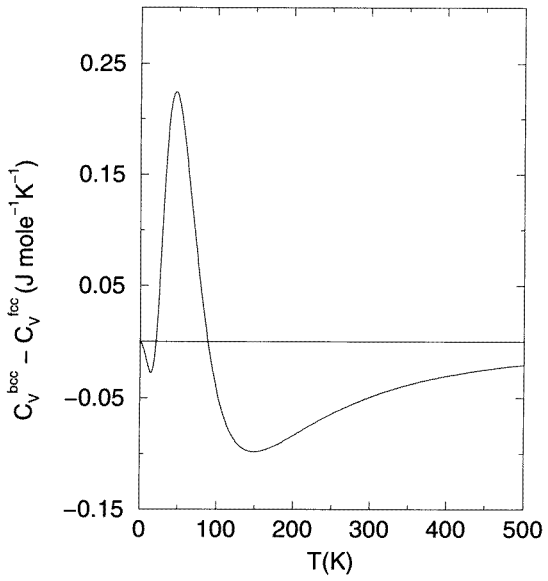

Figure 6. The lattice heat capacity difference between the bcc and fcc structures.

calculated in the harmonic approximation which seems reasonable since we were interested in examining the relative stability of two structures in which the material is known to exist. We were not interested, in this work, in exploring the path/process by which the martensitic transition actually took place, for which anharmonic effects would have been critical. Thus

it would have been satisfying to find that at low temperatures the fcc structure had lower free energy and at higher temperatures the bcc structure was favoured. While we do find the low-temperature result to be appealing, we do not see a crossover of the free-energy curves at around 80 K or so, as suggested from experimental data.

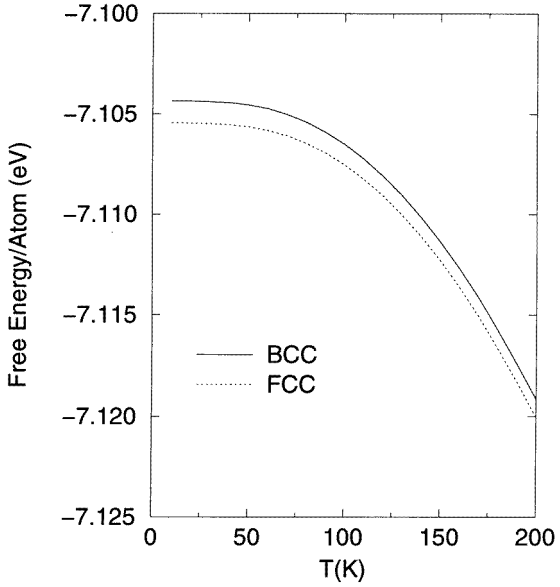

Figure 7. The Helmholtz free energy, $F = F_{vib} + F_{el}$, plotted as a function of temperature.

There are several factors to be considered here. Firstly, we are dealing with energy differences that are of the order of a few meV, which is about the limit of accuracy of the LDA. In this sense even if the two free-energy curves in figure 7 had crossed and the energy differences had remained small, the results would not have been any more conclusive. Secondly, the calculated phonon dispersion curves show an error of about 10% when compared with the experimental values of the modes at the zone boundaries. The experimental values are softer than the calculated ones, in all instances. To test our calculations of the phonon dispersion curves, we have performed similar calculations for bulk phonons in Al, and find an excellent agreement between the measured and calculated phonon dispersion curves along the reported directions in the Brillouin zone. There is, of course, the possibility that an ever-larger value of E_{cut} (>22 Ryd) may produce a better fit to the experimental data for the bcc phonons. At the moment such calculations are beyond our computational powers. There is also the question of the applicability of the pseudopotential approach to lithium which has a large core radius. It will be interesting to compare our results for the phonon dispersion curves to that of an all-electron calculation, but so far such calculations are not available. Thirdly, there is the issue of the accuracy of phonon dispersion curves calculated using the direct method such as here and in reference [13]. As shown in figure 2(b), a rescaling of the phonon frequencies by a factor of 0.9 gives better agreement with the experimental data. What is puzzling is that the Helmholtz free energies calculated with this scaling factor for the phonon frequencies, for both the bcc and fcc structures, do not yield a more conclusive result.

Finally, there is the issue of anharmonic effects. Anharmonic vibrational amplitudes are necessary to bring about any phonon-driven phase transition [42–45, 10]. In an appealing study, Ye *et al* [44] have examined the paths by which Na and Ba undergo martensitic phase transitions. The case of Na is very much akin to that of Li here. The approach taken by these authors is complementary to that in this paper, as it evaluates the possible energy barriers, reaction paths and anharmonic contributions to the vibrational amplitudes. It should be worth pursuing a similar study for Li, which will give more insight into the magnitude of the anharmonic vibrational amplitudes. A fully dynamical study of the martensitic phase transition thus will still have to await further theoretical developments, which will make first-principles molecular dynamics simulations feasible for metallic systems. In the absence of such a study, our conclusion is that the subtle and small energy differences, the long-ranged nature of the ionic interactions, and the presence of a large core radius challenge the applicability of DFT/LDA calculations using *ab initio* pseudopotentials in explaining the dynamics of bulk Li. It is possible that corrections such as the GGA [48] may rectify the problem. We hope that such calculations will be forthcoming.

Acknowledgments

We thank N Chetty, M Weinert and M Rasamni for help with the electronic structure code. TSR would like to thank J Davenport for enticing her to work on electronic structure calculations. This work was supported by the US National Science Foundation under Grant No DMR9120440. Computational resources were provided by the Pittsburgh Supercomputing Center, and by the local Convex Exemplar System which is partially funded by the NSF under grant DMR9413513.

References

[1] Barrett C S and Trautz O R 1948 *Trans. Am. Inst. Mining Metall. Petrol. Eng.* **175** 579
Barrett C S 1956 *Acta Crystallogr.* **9** 671
Barrett C S 1947 *Phys. Rev.* **72** 245
[2] McCarthy C M, Tompson C W and Werner S A 1980 *Phys. Rev.* B **22** 574
[3] Overhauser A W 1984 *Phys. Rev. Lett.* **53** 64
[4] Smith H G 1987 *Phys. Rev. Lett.* **58** 1228
Smith H G, Berlinger R, Jorgensen J D, Nielsen M and Trivisonno J 1990 *Phys. Rev.* B **41** 1231
Ernst G, Artner C, Blaschko O and Krexner G 1986 *Phys. Rev.* B **43** 6465
[5] Schwarz W and Blaschko O 1991 *Phys. Rev. Lett.* **65** 3144
[6] Allen P B and Cohen M L 1969 *Phys. Rev.* **187** 525
[7] Dacorogna M M and Cohen M L 1986 *Phys. Rev.* B **34** 4996
[8] Liu A Y and Cohen M L 1991 *Phys. Rev.* B **44** 9678
[9] Ashcroft N W 1989 *Phys. Rev.* B **39** 10 552
[10] Gooding R J and Krumhansl J A 1988 *Phys. Rev.* B **38** 1695
[11] Bajpai R, Ono M, Ohno Y and Toya T 1975 *Phys. Rev.* B **12** 2194
[12] Wang Y R and Overhauser A W 1986 *Phys. Rev.* B **34** 8401
[13] Frank W, Elsässer C and Fähnle M 1994 *Phys. Rev. Lett.* **74** 1791
[14] Dagens L, Rasolt M and Taylor R 1975 *Phys. Rev.* B **11** 2726
[15] Perdew J P and Vosko S H 1976 *J. Phys. F: Met. Phys.* **6** 1421
[16] Weilacher K H, Roth-Seefrid H and Bross H 1977 *Phys. Status Solidi* b **80** 137
[17] Day R S, Sun F, Cutler P H and King W F III 1977 *J. Phys. F: Met. Phys.* **7** L169
[18] Singh N and Yadav B S 1993 *Physica* **192** 205
[19] Zener C 1947 *Phys. Rev.* **71** 846
[20] Friedel J 1974 *J. Physique* **35** L-59
[21] Animalu A 1967 *Phys. Rev.* **161** 445
[22] Harrison W A 1966 *Pseudopotentials in the Theory of Metals* (New York: Benjamin)

[23] Toya Y 1965 *Lattice Dynamics* ed R F Wallis (New York: Pergamon) p 91
[24] Ihm J, Zunger A and Cohen M L 1979 *J. Phys. C: Solid State Phys.* **12** 4409
[25] Hohenberg P and Kohn W 1964 *Phys. Rev.* B **136** 864
[26] Kohn W and Sham L J 1965 *Phys. Rev.* A **140** 1133
[27] For a review see:
Payne M, Teter M, Allan D, Arias T and Joannopoulos J 1992 *Rev. Mod. Phys.* **64** 1045
[28] Car R and Parrinello M 1985 *Phys. Rev. Lett.* **55** 2471
[29] Chetty N, Weinert M, Rahman T S and Davenport J W 1995 *Phys. Rev.* B **52** 6313
[30] Pickett W E 1989 *Comput. Phys. Rep.* **9** 115
[31] Vosko S H, Wilk L and Nusair M 1980 *Can. J. Phys.* **58** 1200
[32] Troullier N and Martins J L 1991 *Phys. Rev.* B **43** 1993
[33] Louie S G, Froyen S and Cohen M L 1982 *Phys. Rev.* B **26** 1738
[34] Monkhorst H J and Pack J D 1976 *Phys. Rev.* B **13** 5188
[35] Weinert M and Davenport J W 1992 *Phys. Rev.* B **45** 13 709
[36] Kunc K 1984 *Electronic Structure, Dynamics, and Quantum Structural Properties of Condensed Matter* ed J Devreese and P Van Camp (New York: Plenum)
[37] Hellmann H 1937 *Einfuhrung in die Quantumchemie* (Leipzig: Deuticke)
Feynman R P 1939 *Phys. Rev.* **56** 340
[38] Wei S and Chou M 1992 *Phys. Rev. Lett.* **69** 2799
[39] Srivastava G P 1990 *The Physics of Phonons* (Bristol: Hilger)
[40] Boettger J C and Trickey S B 1985 *Phys. Rev.* B **32** 3391
[41] *Phonon States of Elements. Electron States and Fermi Surfaces of Alloys (Landolt–Börnstein New Series)* 1981 Group III, vol 13a, ed K-H Hellwege and J L Olsen (Berlin: Springer)
[42] Kerr W C, Hawthorne A M, Gooding R J, Bishop A R and Krumhansl J A 1992 *Phys. Rev.* B **45** 7036
[43] Ye Y Y, Chan C T and Ho K M 1991 *Phys. Rev. Lett.* **66** 2018
[44] Ye Y Y, Chan C T, Ho K M and Harmon B N 1990 *Int. J. Supercomput. Appl.* **4** 111
[45] Beg M M and Nielsen M 1976 *Phys. Rev.* B **14** 4266
[46] Kittel C 1996 *Introduction to Solid State Physics* 7th edn (New York: Wiley)
[47] Murnaghan F D 1994 *Proc. Natl Acad. Sci. USA* **30** 244
[48] Perdew J P, Chevary J A, Vosko S H, Jackson K A, Pederson M R, Singh D J and Fiolhais C 1992 *Phys. Rev.* B **46** 6671